Journal of Alloys and Compounds 506 (2010) 673–677

Contents lists available at ScienceDirect

Journal of Alloys and Compounds

journal homepage: www.elsevier.com/locate/jallcom

n-Type polycrystalline (CdZn)Se photoelectrode synthesis and its photoelectrochemical characterizations

P.A. Chate [a,*], P.P. Hankare [b], D.J. Sathe [c]

[a] Department of Chemistry, J.S.M. College, Alibag (M.S.), India
[b] Solid State Research Laboratory, Department of Chemistry, Shivaji University, Kolhapur (M.S.), India
[c] Department of Chemistry, KIT's Engineering College, Kolhapur (M.S.), India

ARTICLE INFO

Article history:
Received 1 June 2010
Received in revised form 4 July 2010
Accepted 7 July 2010
Available online 15 July 2010

Keywords:
Chemical bath deposition
Photoelectrochemical cell
Fill factor
Spectral response

ABSTRACT

$Cd_{1-x}Zn_xSe$ photoelectrode have been synthesized by chemical bath deposition method. (CdZn)Se photoelectrode acts as photoanode. The cell configuration is n-CdZnSe|NaOH (1 M) + S (1 M) + Na_2S (1 M)|$C_{(graphite)}$. It is found that fill factor and efficiency are maximum for $Cd_{0.9}Zn_{0.1}Se$. This is due to low resistance, high flat band potential, maximum open circuit voltage as well as maximum short circuit current. The lighted ideality factor was found to be minimum for $Cd_{0.9}Zn_{0.1}Se$ photoelectrode. A cell utilizing photoelectrode showed a wider spectral response.

1. Introduction

In last decade, construction of PEC cells with the aid of active semiconductor–electrolyte junction has been advanced as an alternative to well-known method of energy conversion involving the use of solid state semiconductor solar cells. The alternative method was searched because the usual solar cells are manufactured from highly pure and perfect crystalline materials and p–n junction is obtained using sophisticated technology. For this reason they are quite costly [1–2]. Simple in construction, absence of lattice mismatch, possibility of adjustment of Fermi level by suitably choosing redox electrolyte, no requirement of coating are the advantage of these cells. Semiconductor–electrolyte interface may be used for photoelectrolysis, photocatalysis and photoelectrochemical power generation [3–5]. The direct conversion of solar energy into electrical current using semiconductor–electrolyte interface was first demonstrated by Gerischer [6] and Eills et al. [7]. Since then a large number of metal as well as mixed chalcogenide and oxides have been used as photoelectrode in PEC cells. The stability and efficiency of PEC cells are mainly dependent on preparation conditions for photoelectrode, electrolyte and experimental conditions set during the experiment [8]. Determination of electronic parameters of these semiconducting thin films is essential in testing their suitability. The basic requirements of good thin film photoelectrode for PEC cells are low resistivity and larger grain size. Large grain size leads to reduction of grain boundary area of the thin film leading to an efficient energy conversion. The low resistivity of the photoelectrode required to minimize the series resistance of the PEC cell which leads to lower the short circuit current [9,10]. In PEC cells, the use is made of the interface which is formed on merely dipping the semiconductor into electrolyte solution and liquid junction potential barrier can be easily set up. Polycrystalline semiconductor film can be used without any drastic decrease in efficiency. This is because of the intimate and perfect contact of liquid electrolyte within crystalline grains. Thus PEC cell provide an economical chemical route for trapping solar cells. It consists of a photosensitive n-or-p- type semiconductor electrode and a counter electrode dipped in a suitable electrolyte. Binary and ternary chalcogenide semiconductors of II–VI have received widespread interest in the field of PEC. Single crystals as well as polycrystalline thin films are giving good response.

In previous communication, we reported the successful deposition of polycrystalline CdZnSe thin films by chemical bath deposition technique. Growth mechanism, structural, morphological, compositional, optical, electrical and thermoelectrical properties are studied [11]. This paper deals with photoelectrochemical performance of (CdZn)Se thin film. *I–V*, *C–V* characteristics in dark, power output curves, barrier height measurements, photoresponse, spectral response study.

* Corresponding author. Tel.: +91 0231 2692258.
E-mail addresses: pachate04@rediffmail.com, pachate09@rediffmail.com (P.A. Chate).

0925-8388/$ – see front matter © 2010 Elsevier B.V. All rights reserved.
doi:10.1016/j.jallcom.2010.07.040

2. Experimental details

2.1. Preparation of $Cd_{1-x}Zn_xSe$ photoelectrode

$Cd_{1-x}Zn_xSe$ ($0 < x < 1$) was deposited onto the smooth polished stainless steel substrate, which acts as photoelectrode. The deposition of a typical $Cd_{0.5}Zn_{0.5}Se$ photoelectrode was made in a reactive solution obtained by mixing of, 5 mL(0.2 M) cadmium sulphate octahydrate, 5 mL(0.2 M) zinc sulphate, 2.5 mL (1 M) tartaric acid, 25 mL (2%) hydrazine hydrate and 10 mL (0.2 M) sodium selenosulphate. Sodium selenosulphate was prepared by the following the method reported earlier [12]. All the chemicals used were of AR grade. The total volume of the reaction mixture was made to 150 mL by adding double distilled water. The beaker containing reactive solution was transferred to ice bath of 278 K. The pH was found to be 12.00 ± 0.05. Four-stainless steel substrate were kept vertically in a reaction mixture and rotated with a speed of 50 ± 2 rpm. The temperature of the solution was allowed to rise slowly to room temperatures. The substrates were removed from the beaker after 240 min.

Similar procedure was adapted to synthesis $Cd_{1-x}Zn_xSe$ ($0.1 \leq x \leq 0.9$) thin films. The solutions of cadmium sulphate, zinc sulphate, sodium selenosulphate were mixed in the required stoichiometric ratio of $(1-x):x$:1. The pH of the reactive solution was kept in the range 11.75–12.50.

2.2. Fabrication of PEC Cell

It consists of H-shaped glass tube. One of the arm of the tube was made from hard glass having diameter of size 2.7 cm and length 7 cm and other is ordinary test tube of inner diameter 1.5 cm and length 7 cm. This H-shaped glass container was fitted in a copper pot. A window having the dimension of 2 cm × 1.5 cm was made available for illumination of the photoelectrode. The cell can be represented as:

$$n\text{-}CdZnSe|NaOH(1\,M) + S(1\,M) + Na_2S(1\,M)|C_{(graphite)}$$

Counter electrode is constructed using a graphite rod sensitized in a medium containing concentrated CoS solution for 24 h. A rubber cork was used to make the cell air tight and to support both the counter and photoelectrode. The active area of the size 1 cm × 1 cm was exposed to light. The remaining part of the film was masked by the use of common epoxy resin.

2.3. Characterization of PEC Cell

To study the charge transfer mechanism occurring across the semiconductor–electrolyte interface, the electrical characterization of the PEC cell was tested. *I–V*, *C–V* characteristics in dark, measurement of built-in-potential and power output characteristics under illumination were studied. A wire wound potentiometer was used to vary the voltage across the junction and current flowing through the junction was measured with a current meter. The same circuit was used to determine the capacitance of the junction. The barrier height was examined from temperature dependence of reverse saturation current at different temperature; the lighted ideality factor was calculated. The junction ideality for all the cells were determined by plotting the graph of log*I* versus *V*. Photoelectrochemical activities were studied under 30 mW/cm^2 light illumination. The illumination intensity was measured with Meco Lux meter.

Photoresponse for all the samples were measured to determine the light ideality factor. The short circuit current and open circuit voltage were measured as a function of incident light intensity. Spectral response was determined by measuring the short circuit current as well as open circuit voltage as a function of incident wavelength (400–900 nm).

3. Result and discussion

The nature of contact of the photoelectrode with substrate was examined for all samples. The nature of contact of the photoelectrode with substrate was examined for all samples.

3.1. Electrical properties

3.1.1. I–V characteristics in dark

Current–voltage (*I–V*) characteristics of the PEC have been studied at 303 K. The polarity of this dark voltage was negative towards the semiconductor electrode. After illumination of the junction, the magnitude of voltage increases with increase in negative polarity towards the thin film. The sign of this photovoltage gives the conductivity type of $Cd_{1-x}Zn_xSe$. This indicates that $Cd_{1-x}Zn_xSe$ is a n-type conductor. In the present investigation, symmetrical factor was found to be greater than 0.5 for all compositions suggesting the rectifying nature of the interface [13]. The dynamic current–voltage characteristics are shown in Fig. 1. The junction ideality factor (n_d) can be determined from the plot of log*I* with voltage (*V*) and the variation is shown in Fig. 2. Linear nature of plot was used for the estimation of junction ideality factor. The junction ideality factor was found to be minimum for $x = 0.1$ composition. The higher values of n_d suggest the dominance of series resistance as well as the structural imperfection induced by dissimilarity in the Cd and Zn atomic size and their resulting arrangement in the solid during lattice construction. Defect levels, introduced in this manner inside the valance band and energy gap acts as carrier traps or recombination centers. The junction ideality has a minimum value for $x = 0.1$ suggesting lowest trap density at the photoelectrode–electrolyte interface [14].

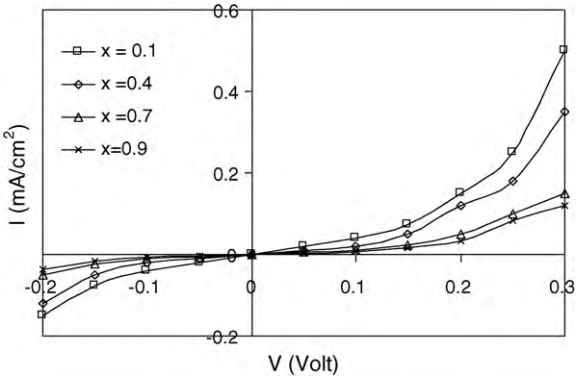

Fig. 1. Current–voltage characteristics of $Cd_{1-x}Zn_xSe$ photoelectrode (in dark).

3.1.2. C–V characteristics in dark

The measurements of capacitance as a function of applied dc bias provided useful information such as type of conductivity and values of flat band potential (V_{fb}) and donor density, band bending depletion layer width position of bond edges, etc. The charge space layer capacitance was measured under reverse biased condition and the flat band potential is obtained from the Mott–Schottky plot. The variation of C^{-2} with voltage for representative samples is shown in Fig. 3. Intercepts of plots on voltage axis determine the flat band potential value of the junction. The flat band potential value enhanced negativeness up to zinc concentration $x = 0.1$, thereafter it decreases. The plot suggests the presence of two regions, which are attributed to the defect structure and surface states present in the $Cd_{1-x}Zn_xSe$ thin film. It also suggests that the junctions are graded type. The plot of flat band potential with composition is shown in Fig. 4. The increase in flat band parameter at $x = 0.1$ is due

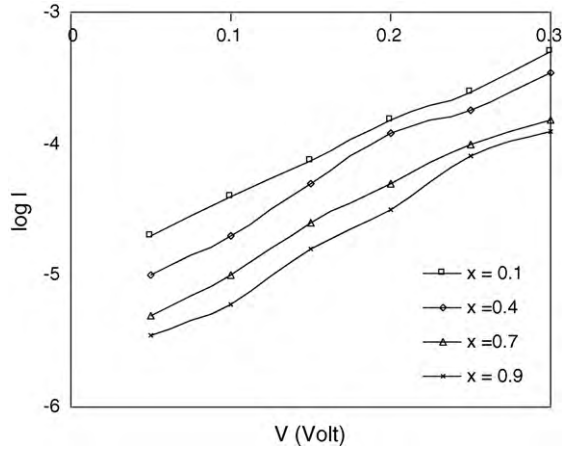

Fig. 2. Plot of log*I* with voltage of $Cd_{1-x}Zn_xSe$ cells.

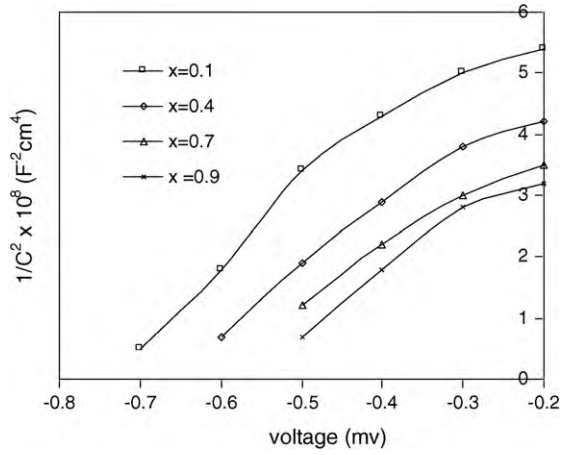

Fig. 3. $1/C^2$ versus d.c. bias voltage of $Cd_{1-x}Zn_xSe$ cells.

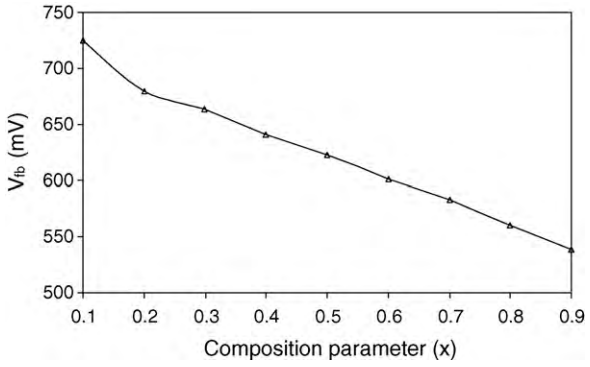

Fig. 4. Plot of V_{fb} against composition parameter (x).

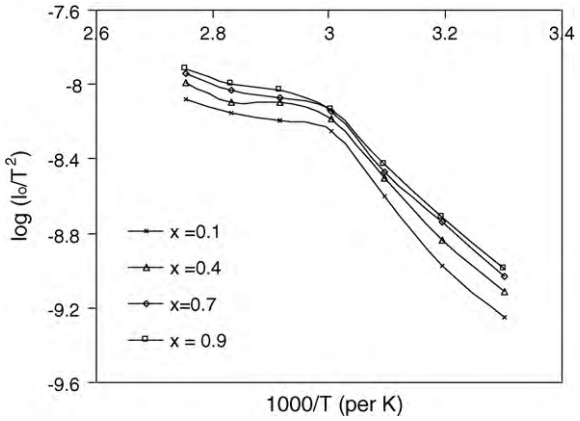

Fig. 5. Plot of $\log(I_o/T^2)$ with $1000/T$ $Cd_{1-x}Zn_xSe$ cells.

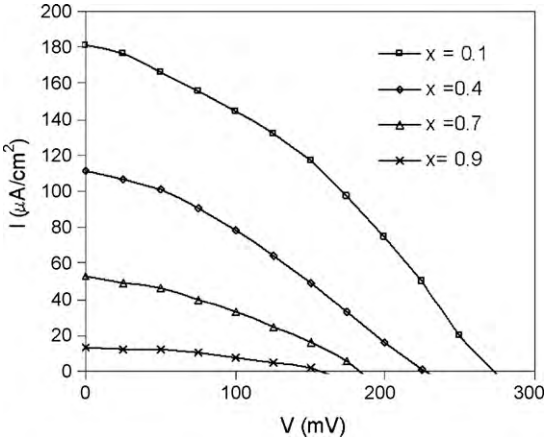

Fig. 6. Power output curves for $Cd_{1-x}Zn_xSe$ photoelectrode.

to decrease electron affinity on addition of Zn^{2+} ions in the lattice of CdSe, an increased amount of surface adsorption and creation of new donor level which shits the Fermi level increasing the amount of band bending.

3.1.3. Barrier-height measurement

The barrier-height was determined by measuring the reverse saturation current (I_o) through the junction at different temperature from 363 to 303 K. The reverse saturation current flowing through junction is related to temperature as [15,16]:

$$I_0 = AT^2 \quad \exp\left(\frac{\Phi_\beta}{kT}\right) \tag{1}$$

where A is Richardson constant, k is Boltzmann constant, Φ_β is the barrier-height in eV. To determine the barrier-height of the photoelectrode, a graph of $\log(I_o/T^2)$ with $1000/T$ was plotted. The plot of $\log(I_o/T^2)$ with $1000/T$ for representative sample is shown in Fig. 5. From the slope of the linear region of plots, the barrier-height was determined. The barrier-height value increases up to $x = 0.1$ (0.192 eV) then decreases.

3.1.4. Power output characteristics

Fig. 6 shows the photovoltaic power output characteristics of various cells were recorded under 30 mW/cm^2 illumination intensity. The various cell parameters like open circuit voltage (V_{oc}), short circuit current (I_{sc}), fill factor (ff), series resistance (R_s), shunt resistance (R_{sh}) and conversion efficiency (η) was determined.

The open circuit voltage, short circuit current, fill factor and efficiency increase up to $x = 0.1$, but decrease thereafter. The series resistance and shunt resistance decreases up to $x = 0.1$, but increases thereafter. The open circuit voltage and short circuit current are found to be 270 mV and 181 μA, respectively. The calculations show that the fill factor is 37.99% and conversion efficiency is 0.61% at $x = 0.1$.The efficiency of CdSe photoelectrode was found to be 0.138% [17]. Similarly, for ZnSe photoelectrode it was 0.13% [18]. $Cd_{0.9}Zn_{0.1}Se$ is better photoelectrode than CdSe and ZnSe photoelectrode. The variation of I_{sc} and V_{oc} with composition parameter is shown in Figs. 7 and 8. At $x = 0.1$, the flat band potential value is

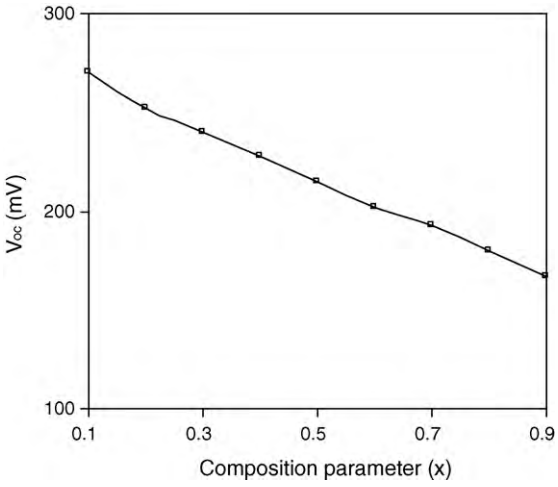

Fig. 7. Plot of V_{oc} with composition parameter.

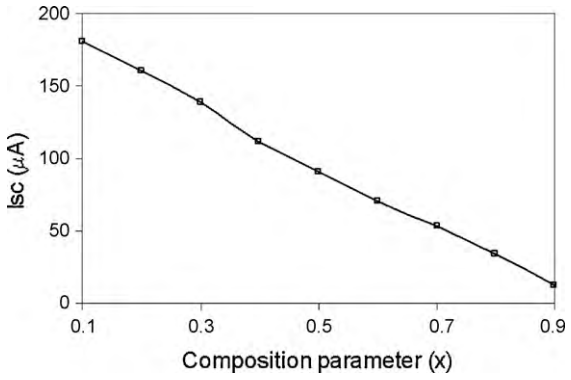

Fig. 8. Plot of I_{sc} with composition parameter.

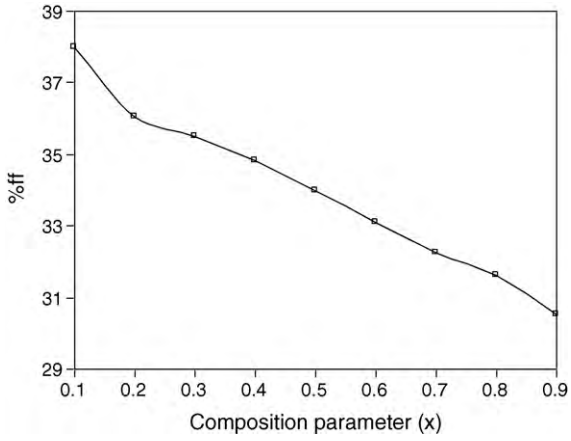

Fig. 9. Plot of %fill factor with compositional parameter.

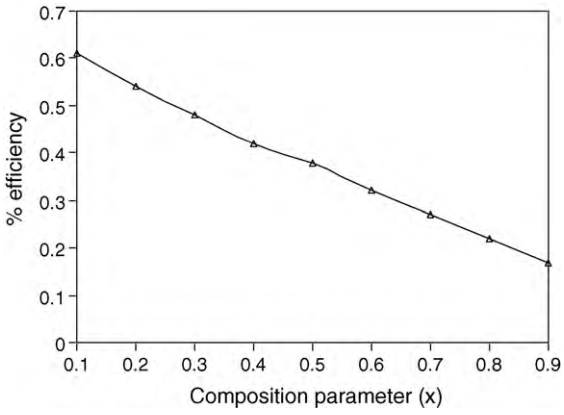

Fig. 10. Plot of % efficiency with compositional parameter.

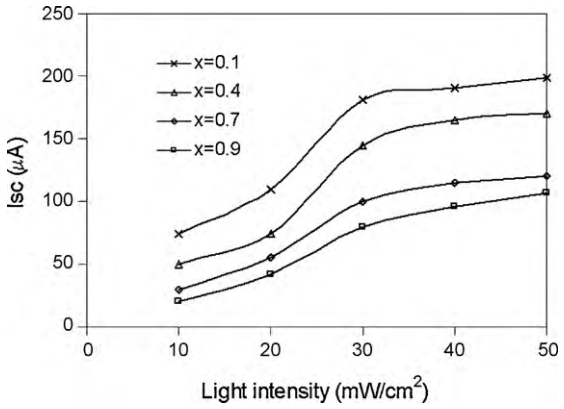

Fig. 11. Plot of I_{sc} with light intensity of $Cd_{1-x}Zn_xSe$ photoelectrode.

more negative as well as comparative band gap, results in enhancement in power efficiency. The high short circuit current was due to decreased photoelectrode resistance and increased the absorbance by the material. The improvement in open circuit voltage was due to increase in flat band potential. The low efficiency in the present investigation might be due to the high series resistance of the PEC cell, low thickness of the film and interface states which are responsible for the recombination mechanism [19]. The series resistance and shunt resistance were calculated from the slope of the power output characteristics using the relation:

$$\left(\frac{dI}{dV}\right)_I = 0 = \frac{1}{R_s} \tag{2}$$

$$\left(\frac{dI}{dV}\right)_{V=0} = \frac{1}{R_{sh}} \tag{3}$$

The values of R_s and R_{sh} were found to be 770 and 500 Ω, respectively. The main drawback in utilizing PEC cell is the absence of space change region at the photoelectrode–electrolyte interface. In this situation, the photogenerated charge carriers can move in both the direction. Lu and Kamat [20] reported that the photogenerated electrons in n-type material either recombine readily with holes or leak out into the electrolyte, instead of flowing through external circuit. The variation of fill factor and efficiency with compositional parameter (x) is shown in Figs. 9 and 10, respectively.

3.2. Optical characterization

3.2.1. Photoresponse

The open circuit voltage and short circuit current were measured as function of light intensity. Fig. 11 shows variation of I_{sc} as a function of light intensity, whereas, Fig. 12 shows the variation of V_{oc} as a function of light intensity. The photoresponse measurements showed a logarithmic variation of open circuit voltage with the incident light intensity. However, at higher intensities, saturation in open circuit voltage was observed, which can be attributed to the saturation of the electrolyte interface, charge transfer and non-equilibrium distribution of electrons and holes in the space charge region of the photoelectrode. But short circuit current follows almost a straight-line path. A plot of $\log I_{sc}$ against V_{oc} should give a straight line and from the slope of the line the lighted ideality factor can be determined. The plot of $\log I_{sc}$ with V_{oc} for representative $Cd_{1-x}Zn_xSe$ photoelectrode is shown in Fig. 13. The lighted ideality factor was calculated for all the photoelectrodes and found

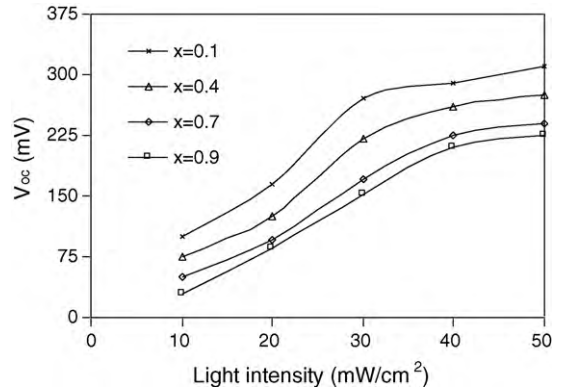

Fig. 12. Plot of V_{oc} with light intensity of $Cd_{1-x}Zn_xSe$ photoelectrode.

Table 1
Various performance parameter of $Cd_{1-x}Zn_xSe$ photoelectrode.

Composition	V_{oc} (mV)	I_{sc} (μA)	η%	ff%	Φ_β (eV)	V_{fb} (V)	R_{sh} (Ω)	R_s (Ω)	n_L	n_d
$Cd_{0.9}Zn_{0.1}Se$	270	181	0.61	37.99	0.192	0.725	500	770	3.91	2.94
$Cd_{0.8}Zn_{0.2}Se$	252	160	0.54	36.03	0.188	0.680	542	825	4.12	3.05
$Cd_{0.7}Zn_{0.3}Se$	240	139	0.48	35.50	0.185	0.664	583	872	4.26	3.15
$Cd_{0.6}Zn_{0.4}Se$	228	111	0.42	34.82	0.181	0.641	616	928	4.53	3.23
$Cd_{0.5}Zn_{0.5}Se$	215	91	0.38	34.00	0.178	0.623	674	1026	4.95	3.33
$Cd_{0.4}Zn_{0.6}Se$	202	71	0.32	33.10	0.176	0.601	726	1126	5.19	3.46
$Cd_{0.3}Zn_{0.7}Se$	193	53	0.27	32.26	0.174	0.583	829	1359	5.57	3.59
$Cd_{0.2}Zn_{0.8}Se$	180	34	0.22	31.60	0.173	0.560	992	1532	5.79	3.68
$Cd_{0.1}Zn_{0.9}Se$	167	13	0.17	30.50	0.172	0.539	1159	1783	6.12	3.78

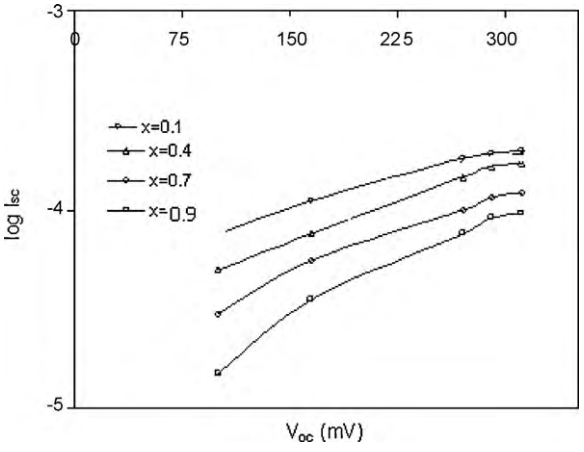

Fig. 13. Plot of log I_{sc} with V_{oc} for $Cd_{1-x}Zn_xSe$ photoelectrode.

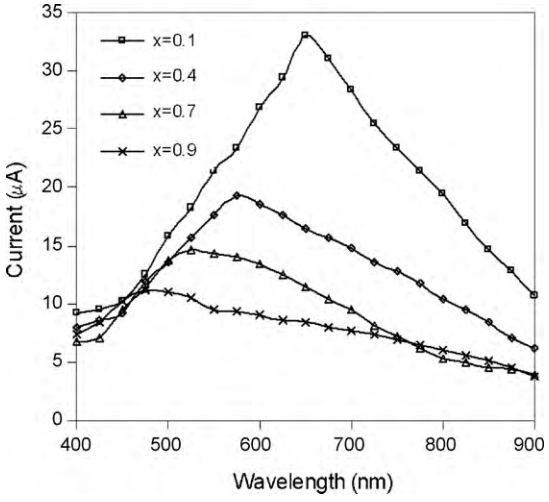

Fig. 14. Plot of I_{sc} with wavelength for $Cd_{1-x}Zn_xSe$ photoelectrode.

to be minimum for $Cd_{0.9}Zn_{0.1}Se$ composition. The observed value being 2.94 for $x = 0.1$ photoelectrode.

3.2.2. Spectral response

The spectral response of a cell has been recorded in 400–900 nm wavelength range. The photocurrent action spectra were examined and are shown in Fig. 14 It is seen that spectra attains maximum value of current at $\lambda = 650$ nm for $Cd_{0.9}Zn_{0.1}Se$ photoelectrode decreases with increase in wavelength. The decrease of current on shorter wavelength side may be due to absorption of light in the electrolyte and high surface recombination of photogenerated minority carriers [21]. The decrease in current on longer wavelength side may be attributed to non-optimized thickness and transition between defect levels [9]. The maximum current is obtained corresponding to $\lambda = 650$ nm gives band gap value 1.90 eV for $Cd_{0.9}Zn_{0.1}Se$ agreeing with the results of optical absorption studies [11].

The various cell characteristics such as V_{oc}, I_{sc}, η%, ff%, Φ_β, V_{fb}, R_s, R_{sh}, n_L, n_d are cited in Table 1 for $Cd_{1-x}Zn_xSe$ photoelectrode.

4. Conclusions

The PEC cell can be easily fabricated using $Cd_{1-x}Zn_xSe$ photoanode sulphide-polysulphide as electrolyte, CoS treated graphite rod as a counter electrode. A saturated calomel electrode was used as reference electrode. The various performance parameters were determined with respect to the composition parameter (x). It is found that the fill factor and efficiency is maximum for $Cd_{0.9}Zn_{0.1}Se$ composition.

References

[1] S. Pass, Y.S. Chaudhary, M. Agrawa, A. Shrivastav, R. Shrivastav, V.R. Satsangi, Ind. J. Phys. 78A (2004) 229.
[2] M. Ramrakhiani, Physics News (September–December) (1998) 115.
[3] B. Miller, A. Heller, M. Robbins, S. Mebzones, K.C. Change, J. Thomson, J. Electrochem. Soc. 124 (1977) 1019.
[4] M.T. Gurierrez, J. Ortega, Electron. Sol. Energy. Mater. 20 (1990) 387.
[5] P.J. Holes, The Electrochemistry of Semiconductors, Academic Press, 1992.
[6] H. Gerischer, Electrochemistry 58 (1975) 263.
[7] A.D. Eills, S.W. Kaiser, M.S. Wrighton, J. Phys. Chem. 80 (1976) 1325.
[8] C.D. Lokhande, Solar Cells 22 (1987) 133.
[9] V.V. Killedar, C.D. Lokhande, C.H. Bhosale, Indian J. Pure Appl. Phys. 36 (1998) 643.
[10] D. Das, Proc. Conf. Phys. Tech. Semicond. Dev. Integr. Circuits 1523 (1992) 323.
[11] P.P. Hankare, P.A. Chate, M.R. Asabe, S.D. Delekar, I.S. Mulla, K.M. Garadkar, J. Mater. Sci. Mater. Electron. 17 (2006) 1055.
[12] A. Darkowski, A. Grabowski, Sol. Energy Mater. 23 (1989) 75.
[13] L.P. Deshmukh, Indian J. Pure Appl. Phys. 36 (1998) 302.
[14] A.M.A. Dhafiri, A.A.I. Al-Bassam, Sol. Energy Mater. Sol. Cells 33 (1994) 177.
[15] M.A. Butler, J. Appl. Phys. 48 (1977) 1914.
[16] A. Aruchami, G. Aravamudan, G.V. Subba Rao, Bull. Mater. Sci. 4 (1982) 483.
[17] A.A. Yadav, M.A. Barote, E.U. Masumdar, Chalcogenide Lett. 6 (2009) 149.
[18] P.P. Hankare, P.A. Chate, P.A. Chavan, D.J. Sathe, Alloys Compd. 46 (2008) 623.
[19] K.Y. Rajpure, S.M. Bamane, C.D. Lokhande, C.H. Bhosale, Indian J. Pure Appl. Phys. 37 (1999) 413.
[20] D. Lue, P. Kamat, J. Phys. Chem. 97 (1993) 1073.
[21] H. Gerischer, Electron. Anal. Chem. 150 (1983) 553.